

# On a design of a torque sensor for the iCub humanoid robot

Wiktoria Sieklicki, Francesco Becchi

Telerobot, Genova, Italy

wiktoria.sieklicki@gmail.com, becchi@telerobot.it

## Abstract

The paper presents the evaluation process of a first version of the one axis torque sensor designed for the iCub humanoid robot. Newly designed strain gauges equipped sensor was found to show a significant readouts hysteresis, therefore several tests were run to define the reason of the hysteresis. Some of the design issues met while testing the new sensor are discussed including the screws connection and relative rigidity of the sensor's elements analyses. Verification of the assembly procedure is also included. Tests revealed several problems on both design stage and exploitation of the sensor. Possible solutions to the encountered problems are further proposed.

**Index Terms:** torque sensor, strain gauge, friction, fatigue analysis

## 1. Introduction

A humanoid robot low-level understanding of the environment is provided by the sensors in which it is equipped. Interaction with the real objects and moving within the unspecified environment is only possible, when adequate amount of information is provided. This include external and internal forces and torques applied to the robot's end-effectors which in case of the iCub robot have been sensed with use of four 6-axis Force/Torque sensors placed along the kinematic chain of legs and arms – one sensor in each [1]. Information from those sensors, together with on-fly motor current measurements has been insufficient though for the robot to walk. More detailed information about the torques applied by each motor of the robot can be provided by a joint level torque sensors what shall result in better understanding of the internal and external forces of the manipulators and shall widen the robot's possibilities to interact with the environment [2]. The joint torque level control offers moreover possibility to compensate effects of the robot dynamics without real time computation of the robot dynamics and the control schemes may be robust in respect to parameter variations [3,4]

A single-axis torque sensors were considered to be placed in each powering unit of the robot's lower-body (Fig.1, left). In powering units B to F one torque sensor was considered, whereas since powering unit A consists of four motors, this part was assigned with four torque sensors. Because the iCub robot is very compact, the torque sensor had to be designed specifically for this application with several design limitations imposed. [5]. The torque sensor (Fig.1, e) was considered to be placed in the kinematics chain of each powering unit of the robot after the harmonic drive CSD-17-100 flexspline (Fig.1, c) and before the unit output (Fig.1, a).

Readouts of the newly designed sensor appeared to have a hysteresis though and for this reason a series of sensor's tests were commissioned. This paper presents the evaluation process of a first version of the sensor and discusses some of the sensor's design issues found while testing the sensor. Possible solutions to the encountered problems are also proposed.

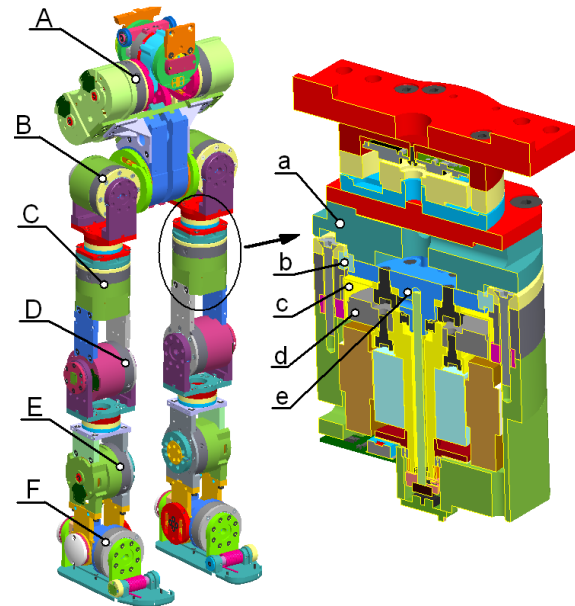


Figure 1: Placement of the 1-axis torque sensors in the iCub robot's structure (left), assembly of a torque sensor (right) – output flange (a), bearing (b), flex spline (c), wave generator (d), sensor (e).

## 2. The sensor

Tested sensor structure was made of 17-4 ph stainless steel characterized by 1100MPa ultimate tensile stress and 200GPa Young modulus[6]. The sensor design involved an inter mounting part constrained to the harmonic drive with use of 6xM4 8.8 screws on a radius of 7.29mm each, an outer mounting hoop constrained with use of 8xM3 8.8 screws on a radius of 17.5mm and four beams out of which two had strain gauges glued onto (Fig.2). All mounting holes in the sensor were threaded with ISO thread. The sensor in the robot assembly was also supported by KAA15XLO bearing on an outer hoop (Fig.1, b).

The sensor was equipped with SS-060-033-500P Micron Instruments P-doped silicon semiconductor bar-type strain gauges of 500Ohms nominal resistance and 0.84mm of active length [2]. Strain gauges were connected in Wheatstone's bridge design employing four strain gauges arranged in a two half-bridges configuration.

Readings of the sensors were acquired via the CAN bus by the STRAIN board [3]. The utilized board was designed for a six axis Force-Torque sensor used in the earlier versions of iCub. It operates six Wheatstone half-bridges equipped with very same strain gauges as in discussed application, on six independent channels. For sake of this study, only two channels were utilized. To acquire data from the STRAIN board a Canreal software ver. 4.33 was used. Data was displayed with use of Gulp! software ver.0.22 alpha. Offset was set with help of the Gulp! software.



Figure 2: Sensor structure (left) - inner mounting part (a), outer mounting hoop (b), sensor beams (c), short beams (d); strain gauges glued onto the sensor (right).

### 3. Tests setup

In order to provide most uniform testing conditions special mounting flanges were manufactured. Inner mounting flange was simulating connection with a harmonic drive and was constrained to the table, whereas an outer flange was designed in the way to enable application of a constant torque to the sensor. Sensor was then fixed to the mounting flanges with screws. Torque was applied by loading a rod having 287mm of length in the way, that the load vector was in the plane of the sensor's face surface and perpendicular to the radius of the sensor body. To achieve this, weights were hung on a cord at the end of the rod. The sensor was also tested under equal loads applied in opposite directions (creating a pair of forces), but results were comparable to the previously discussed load case, whereas the test setup was far more complicated. Since the radial deflection of the loaded sensor was noticed to be approx.  $0.5^\circ$  it was decided, that the load applied to one of the rods should have given sufficient approximation. Sensor was loaded with loads varying from 1 to 11kg. Maximum torque that the sensor was designed to withstand is 40Nm, what is adequate to the load of 14kg applied on a 287mm long lever. Tests were mostly carried out in the load range of up to 20 Nm because they involved mounting the sensor with some screws loosen what entailed much more stressful load case than provisioned for the sensor. Tests were done in a steady temperature conditions of approximately  $20^\circ\text{C}$  ( $\pm 5^\circ\text{C}$ ). Hysteresis of the sensor's readouts was observed to be independent from the environment temperature.

### 4. Tests

Obvious reason for hysteresis in case of strain gauges is gluing to the bending surface, what may result in some amount of permanent deformation of the loaded glue. Whether this was the reason, the sensor was loaded when not constrained rigidly to anything (with loosen all the screws mounting the sensor). Such a test setup resulted in lack of hysteresis. This proved, that the strain gauges are glued correctly to the sensor body.

Verification procedure was begun with checking the signal conditioning system. Alternative acquisition module (ADT4U-RS232, WoBit production) was used together with dedicated software (ADT4U-PC ver.1.02) in order to verify the correctness of the STRAIN board and software functioning. The new acquisition module was earlier tested with other strain gauges presenting no problems. New setup showed the same drawbacks as the original one. Hence it was deduced, that the sensor readouts problems do not origin from electronics nor software errors. Further tests were carried out with use of the original acquisition module and software.

#### 4.1. Screws connection verification

During initial tests it was observed, that the mounting screws tightening torque was significantly influencing the sensor's readouts hysteresis. Tests of friction based connection (with use of not shoulder screws) shown, that in best case of tightening torques (M4 and M3 screws tightened with 3.5 and 2Nm respectively) residuals of the sensor's readouts were varying from 15 up to 24% of the applied load (Fig.2 - dark blue). Tightening screws with higher torques resulted in higher values of residuals, whereas tightening screws with lower torques improved results for low load values but for high load values it made residuals unacceptable high. Following tests were meant to provide information of which connection element causes most of the problems and if use of shoulder screws does alter the results. Testing was divided in two cases - first involving only inner mounting flange connected with the sensor with tightened screws, whereas the outer hoop was attached to the mounting flange with loosen screws, and the later one involving the external mounting flange connected to the sensor's outer hoop with tightened screws, whereas the inner mounting flange was attached with loosen screws.

Tests involving only outer hoop connected with use of tightened, not shoulder screws (tightening torque: 1 - 2.5Nm) revealed that residuals for different tightening torques and different loads applied varied from 5 to 15% of applied load (Fig.2 - dark green). Best results were achieved for the sensor connected by the outer mounting flange with M3 screws tightened with 2Nm torque. Further tests including only inner mounting flange connected with use of tightened, not shoulder screws (tight. torque:1-4Nm) revealed that the residuals varied for different tightening torques and different loads between 0.2 and 3.4% of applied load (Fig.2 - light red). Best results were achieved for the sensor connected by inner mounting flange with M4 screws tightened with 3.5Nm torque.

At this point it is important to note, that M4 screw 8.8 is able to withstand 6.1kN of axial force before elongating plastically (what is not acceptable). The axial force was therefore considered acceptable if the stress in the screws does not exceed 520 MPa, which is  $0.65 \cdot \text{Ultimate tensile stress}$ . In this case axial force evoked according to Eq.1. in a single screw is 4kN. Tightening torque applied to each screw shall be then 3.48Nm.

$$F_{\text{axial}} = \frac{M}{0.5 \cdot d_2 \cdot \left( \tan \left( \arctg \left( \frac{\mu g}{\cos(\alpha)} \right) + \arctg \left( \frac{P}{\pi \cdot d_2} \right) \right) \right) + 0.5 \cdot dh \cdot \mu} \quad (1)$$

,where  $M$  is a tightening torque,  $d_2$  is a middle diameter of a screw ( $=3.545\text{mm}$ ),  $\mu g$  is a friction coeff. between surfaces of the thread ( $=0.15$ ),  $\alpha$  is a tread's lead angle ( $=0.5236\text{rad}$ ),  $P$  is a tread's pitch ( $=0.7$ ),  $dh$  is a screw's head middle diameter ( $=5.9\text{mm}$ ) and  $\mu$  is a friction between screw's head and a reciprocal surface ( $=0.15$ ). Since the friction between the sensor and the inner mounting flange is directly dependent from the axial force evoked by screws, value of the friction force ( $T$ ) evoked with tightening all six ( $n$ ) screws is calculated according to Eq.2 to be 3.6kN (assuming  $\mu$ , as well as  $\mu_g$  equal 0.15).

$$T = F_{\text{axial}} \cdot n \cdot \mu_g \quad (2)$$

$$M_{\text{friction}} = T \cdot \frac{d}{2} \cdot \mu \quad (3)$$

The momentum of friction ( $M_{\text{friction}}$ ) between the sensor and the rear mounting flange's surfaces - necessary to keep the sensor on its original position - is according to Eq.3 26Nm, where  $d$  is a middle diameter of the surfaces being in contact

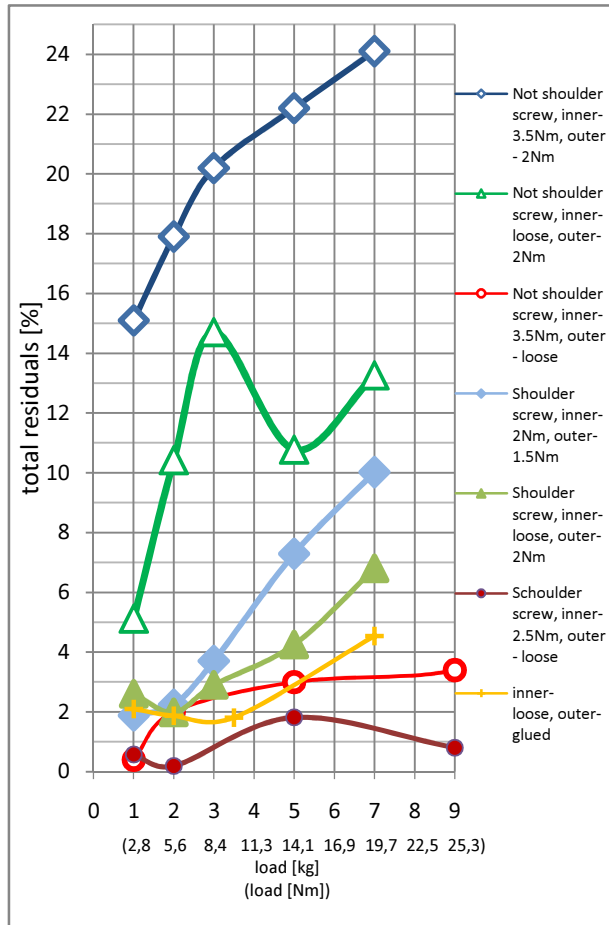


Figure 3: Residuals of the sensor's readouts in percentage of total load applied to the sensor after the load is removed.

(=14.58mm). Calculated friction momentum is less than expected 40Nm, thus relative movement between parts appear.

Similar calculations were done for M3 screws. Axial force in every single screw was assumed to be  $F_{axial}=2.3kN$ , screws tightening torque  $M=1.6Nm$ , middle diameter  $d_2=2.675mm$ , friction coeff.  $\mu_g=0.15$ , thread's lead angle  $\alpha=0.5236rad$ , thread's pitch  $P=0.5$ , screw's head middle diameter  $d_h=5mm$ , friction coeff.  $\mu=0.15$ , number of screws  $n=8$ , middle diameter of surfaces in contact  $d=17.5mm$ . It was calculated, that eight M3 screws provide a 48Nm of friction momentum.

Above numbers does not correspond though with the fact, that tightening M3 screws resulted in much higher hysteresis during tests, what was shown in Fig.2. Screws diameter must had been therefore not the only reason for hysteresis. Shoulder screws were introduced in place of the regular ones in order to minimize the relative movement of sensor and mounting flanges. In this case screws' shafts was supposed to keep the sensor on its position rather than friction between surfaces.

Tests involving shoulder screws shown, that when screws at both inner and outer mounting flanges were tightened, best results were obtained for M3 and M4 screws tightened all with torque of 2 and 1.5Nm respectively. Hysteresis was in such case varying from 2.7 to 7.4% of applied load for different torques applied (Fig.2 - light blue).

Similarly to the previous tests, inner and outer mounting flanges were further investigated separately. Outer loop screwed with eight M3 shoulder screws (tight. torques: 1 - 2.5Nm) resulted in the residuals varying from 1.8 to 7.0% of

applied load for different torques applied to the sensor (Fig.2 - light green). Tests including only inner mounting flange connected with use of six M4 shoulder screws (tight. torques: 1 - 4Nm) revealed that the residuals varied for different tightening torques and different loads from 0.2 to 3.4% of applied load (Fig.2 - dark red).

Another important aspect of the threaded connection is that there should be enough material left around threaded holes to withstand pressure caused by the screw head when tightening the screws. This apply particularly to the M4 screws, since M3 screws' heads do not come into contact with the sensor in the assembly. From the condition for surface pressures (Eq.4), the bulk material around the threaded hole should have a minimal diameter of ( $d_m$ ). Applying axial force of 4kN by each the M4 screw implies having a minimal diameter of 6.25mm of material that has to surround the hole.

$$d_m = \sqrt{\frac{4 * F_{axial}}{\pi * \sigma_k} + D^2} \quad (4)$$

, where  $\sigma_k$  is an ultimate tensile stress (1100MPa) multiplied by a safety coeff. (0.65),  $D$  is an external diameter of a threaded hole. The sensor has bulk material around M4 threaded holes of 5.5mm in diameter, what is not sufficient for the hole to stay undeformed after tightening the screws.

In order to further minimize the hysteresis, the sensor was glued with outer mounting flange (sensor was left attached to the inner m.f with loosen screws). For this reason Epoxy Loctite 9497 A&B Hysol was used. This mounting scheme resulted in significant improvement. In this case hysteresis was varying from 1 to 4.1% of applied load with much less steep characteristics (Fig.2 - orange).

Next candidate to cause the hysteresis was the mismatched relative rigidity of sensor's elements. Finite element analysis was done using ANSYS software in order to evaluate correctness of the sensor's shape design. Particular attention was paid to the external mounting hoop (Fig., b) of the sensor. The reason for investigating this element was that only a deflection of intended elements should be measured by the strain gauges, whereas in this design the rigidity ratio between elements which are supposed to deflect (Fig.2, c and d) and an element which is supposed to stay rigid (Fig.2, a and b) seemed to be too small. For the purpose of this analysis a radial displ. of 0.0189rad was applied to each of the mounting holes of the outer mounting hoop, while inner mounting part was constrained (forces and displacements were applied to all nodes of holes surfaces). Such load case resulted in 637MPa of stress (Fig.4, right). To simplify the representation of displacements, the design was transformed into a Cartesian coordinate system (Fig.5) as an infinite subsequent series of two beams (representing entities c and d from Fig.2) coupled by a thick part from one side and a thin part from the other (which correspond to entities a and b from a Fig.2).

Applying a displacement of  $f=0.032mm$  in Y direction to the same holes as in the case of circular design (what represents a displacement of 0.0189rad applied to the circular design) resulted in maximum stress of 640MPa (Fig.4, bottom). Circular and serial designs shows therefore a good approximation. As an outcome of applied translation along Y axis, a lateral translation of 0.023mm along X axis occurred next to the short beams forcing elements to rotate. Unwilled rotation is a result of too rigid short beam in respect to a coupler. The rotation is caused by internal forces which are shown in Fig.6 - in this case a sensor was constrained by holes of the outer mounting hoop, whereas force was applied to the thick part of the sensor.

In this load case reaction forces in X direction evoked at the holes next to the short beam were 678N and -678N, what was in each case approximately one third of a total force applied in Y direction to the sensor. At the same time reaction forces in Y direction evoked at the holes next to the short beam were 839N. Internal forces in this element behave as a pair of forces applied to the coupler rotating it and causing this way a respective movement between the sensor's external hoop and the mounting flange. Therefore it can be stated, that the external hoop of the sensor was not rigid enough to keep the mounting holes in fixed position in respect to each other.

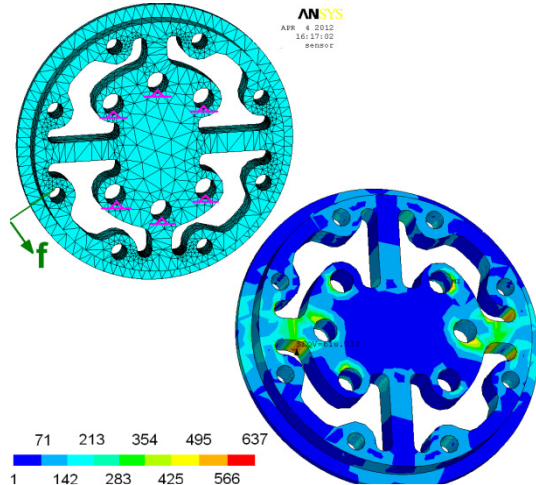


Figure 4: Sensor initial conditions (top) and a stress distribution under  $f=0.0189\text{rad}$  displacement applied to the mounting holes of outer hoop (bottom).

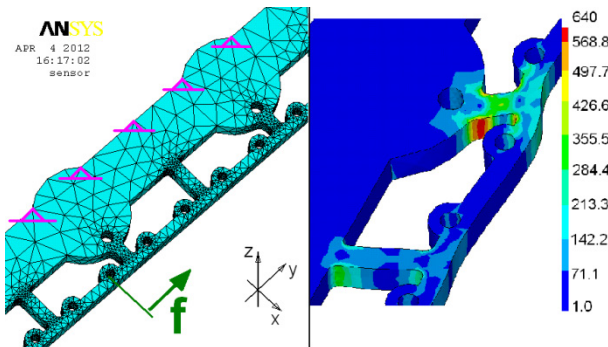


Figure 5: Serial representation of the sensor with analysis initial conditions (left), stress distribution under  $f=0.034\text{mm}$  displacement applied-displacement representation is scaled up 100 times (right).

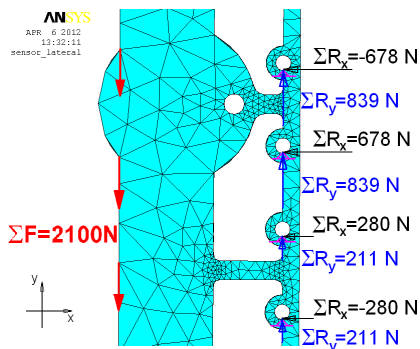


Figure 6: Serial representation of the sensor with internal loads shown.

## 5. Conclusions

Tests of the sensor revealed, that the hysteresis of the sensor's readouts in its original connection scheme was significant and residuals varied from 10 to 24% of the applied load for different torques applied to the sensor. The sensor's connection to the output/input flanges scheme, relying on friction was found to be incorrect - sensor was moving in respect to the mounting flanges when load was applied. The connection should have been designed in the way to provide enough friction between contact surfaces or it should rely on pin connection rather than on the friction. Most important result of presented study was that applying torque to the sensor resulted in deformation of the sensor's outer mounting hoop, what caused relative motion of parts hence the friction. Revision of the sensor's design revealed also that amount of bulk material left around the threaded holes was not sufficient - the sensor deflected upon tightening the mounting screws.

Sensor's tests gave several important hints to minimize the readouts' hysteresis. At the design stage of the sensor it is important to decide on a proper mechanical sensor's interface. For friction based interface friction between elements should be enough to keep them with no respective movement. Screws with calibrated shaft gave most repeatable results with less hysteresis in case of discussed case (residuals varying from 2 to 7.2% of applied load for different torques). It should be kept in mind, that this problem arise in case when some of the mechanical interface elements are not rigid enough to stay undeformed. Kind of solution may be gluing parts together (in this case it resulted in hysteresis 5 to 10 times smaller than in the initial tests with friction based connection). It was also shown, that for a given connection scheme – screw based – it is important to maintain a proper tightening torques of screws. With hand screwdriver human can apply much higher tightening torques than M3 or M4 screws can withstand. This may result in plastic elongation of screws and uncertain behavior of the sensor's mechanical interface.

## 6. Acknowledgements

This research has been supported by the EU FP7 Project RobotDoC ITN (235065 Marie Curie Actions).

## 7. References

- [1] Fumagalli M., Gijsberts A., Ivaldi S., Jamone L., Metta G., Natale L. & Nori F., Learning To Exploit Proximal Force Sensing: a Comparison Approach. In: O. Sigaud & J. Peters (Eds). From Motor to Interaction Learning in Robots, 2010, pp. 159-177
- [2] Stokic D. and Vukobratovic M., Historical perspectives and state of the art in joint force sensory feedback control of manipulation robots, 1993, Robotica, 11:149-157
- [3] Asada H., Youcef-Toumi K., Direct-Drive Robots. 1987, Cambridge, MA: MIT Press
- [4] Kosuge K., Takeuchi H. and Furuta K., Motion control of a robot arm using joint torque sensors. IEEE Transactions on Robotics and Automation, 1990, 6(2):258-263
- [5] Tsagarakis N., Vanderborght B., Laffranchi M., Caldwell D. The mechanical design of the new lower body for the child humanoid robot iCub, IEEE/RSJ International Conference on Intelligent Robots and Systems, 2009, St. Louis, USA, pp. 4962-4968
- [6] [http://www.aksteel.com/pdf/markets\\_products/stainless/p\\_recipitation/17-4\\_PH\\_Data\\_Bulletin.pdf](http://www.aksteel.com/pdf/markets_products/stainless/p_recipitation/17-4_PH_Data_Bulletin.pdf)
- [7] <http://www.microninstruments.com/datasheets/DS-Bar%20Strain%20Gage.pdf>
- [8] [http://eris.liralab.it/wiki/FT\\_sensor](http://eris.liralab.it/wiki/FT_sensor)